Characterizing eye shape with minimum curves

Sitansu Kumar Subudhi

Department of Computer Science and Engineering
National Institute of Technology Rourkela

Characterizing eye shape with minimum curves

Thesis submitted in partial fulfillment

of the requirements of the degree of

Master of Technology

in

Computer Science and Engineering
(*Specialization*: *Computer Science*)

by

Sitansu Kumar Subudhi

(Roll Number: 712CS1154)

based on research carried out

under the supervision of

Prof. Sambit Bakshi

May, 2017

Department of Computer Science and Engineering
National Institute of Technology Rourkela

Department of Computer Science and Engineering
National Institute of Technology Rourkela

Prof. Sambit Bakshi
Assistant Professor

May 30, 2017

Supervisor's Certificate

This is to certify that the work presented in the thesis entitled *Characterizing eye shape with minimum curves* submitted by *Sitansu Kumar Subudhi*, Roll Number 712CS1154, is a record of research carried out by him under my supervision and guidance in partial fulfillment of the requirements of the degree of *Master of Technology* in *Computer Science and Engineering*. Neither this thesis nor any part of it has been submitted earlier for any degree or diploma to any institute or university in India or abroad.

_____
Sambit Bakshi

Declaration of Originality

I, *Sitansu Kumar Subudhi*, Roll Number *712CS1154* hereby declare that this thesis entitled *Characterizing eye shape with minimum curves* presents my original work carried out as a postgraduate student of NIT Rourkela and, to the best of my knowledge, contains no material previously published or written by another person, nor any material presented by me for the award of any degree or diploma of NIT Rourkela or any other institution. Any contribution made to this research by others, with whom I have worked at NIT Rourkela or elsewhere, is explicitly acknowledged in the dissertation. Works of other authors cited in this dissertation have been duly acknowledged under the sections “Reference” or “Bibliography”. I have also submitted my original research records to the scrutiny committee for evaluation of my dissertation.

I am fully aware that in case of any non-compliance detected in future, the Senate of NIT Rourkela may withdraw the degree awarded to me on the basis of the present dissertation.

May 30, 2017
NIT Rourkela

Sitansu Kumar Subudhi

Acknowledgment

I would like to express my heartfelt thanks to my guide, Dr. Sambit Bakshi, for giving me an opportunity to work under him in the area of iris recognition. I owe it to him for providing me with ideas of how to complete this work. I would also like to thank all my friends, who have been a constant source of encouragement for these past five years. Finally, I have no words on how to convey my gratitude towards my parents and my brother. They have always believed in me and it is due to their blessings, I could give my full dedication. —

May 30, 2017
NIT Rourkela

Sitansu Kumar Subudhi
Roll Number: 712CS1154

Abstract

Iris segmentation is an essential module in iris recognition systems. It defines the effective image region used for subsequent processing such as feature extraction and matching, which are related to recognition accuracy. It is one of the most time consuming module in iris recognition. Some of the challenges faced here are specular reflections due to glasses, pupillary and iris boundaries being non-circular, and defocusing, motion blur or poor contrast. Therefore, here in this research work, the segmentation process is carried on the iris images, where we define the outer iris boundary and inner pupil region. It is carried out on the UBIRIS iris image database. The edge map of the iris image is found out using edge detection techniques, which are further used in finding out the eyelids and their intersection points with the outer iris boundaries. We define four such points C1, C2, C3 and C4, where the iris intersects with the eyelids and define the curves joining these points.

***Keywords*: *localization*; *iris segmentation*; *curve fitting*; *eyelid detection*; *edge detection*.**

Contents

List of Figures

List of Tables

Chapter 1

Introduction

The science of confirming and verifying an individual in view of their physical, compound or behavioral properties is known as biometrics. There is a requirement for dependable identity detection frameworks that can suit a substantial number of people. The exactness of these frameworks rely on upon the capacity to precisely decide a person among a few others. General structure of a biometric framework :

i) Obtain raw biometric information from people,

ii) Draw out the most prominent features from the obtained data,

iii) Compare against stored feature sets, and

iv) Execute action based on result.

As discussed in handbook of biometrics[1], there are four primary modules in a non specific biometric framework: sensor module, quality evaluation/feature extraction module, decision making and matching module, and database framework module.

Sensor module : Raw biometric information is be procured by a reasonable biometric device such as scanner. It characterizes the human machine interface and is, thus, crucial to the execution of the biometric framework. Interface outlined of unremarkable quality can bring about a high inability to obtain rate which would bring about low client satisfaction.

Quality evaluation alongwith feature extraction module : Biometric information obtained by the sensor is evaluated with a specific end goal to decide if it can be additionally handled. It is ordinarily subjected to any enhancement method keeping in mind the end goal to enhance its quality. An arrangement of most prominent features is extracted and stacked away as template(during enlistment) to be interpreted as trait of the individual.

Decision making and matching module : The drawn out elements are contrasted against the stacked away formats which creates match scores. Match scores are utilized to either approve a guaranteed personality or give a positioning of the enlisted characters all together to distinguish a person.

Database framework module : The database is a place where we store all biometric data which may include name, phone numbers, addresses, and so forth.) portraying the client.

Biometric characteristics

Any human physiological as well as behavioral trademark can be utilized as a biometric

trademark the length of it fulfills the accompanying prerequisites:

1. Universal - Each individual ought to have the characteristic.
2. Uniqueness - The offered biometric to be distinctive crosswise over people in the populace.
3. Perpetual quality or permanency - The biometric ought not change over a timeframe.
4. Quantifiability - It should be conceivable to procure and digitize the biometric quality utilizing reasonable gadgets and not bother the person.
5. Performance execution - The system accuracy ought to meet the requirements forced by the application.
6. Agreeableness - Individuals should not be coerced to submit their biometric attribute to the framework.
7. Circumvention - the straightforwardness with which the characteristic of a person can be imitated

1.1 Anatomy of human eye

The iris is the ring like area of the eye limited by the sclera, which is the white of the eye and the pupil on either side. It between the cornea and the focal point of the human eye. The iris is punctured near its inside by a roundabout gap known as the pupil. The purpose of the iris is to moderate the measure of light entering through the pupil, and this is finished by the sphincter and the dilator muscles, which alter the measure of the pupil. The normal radius of the iris is 6 mm, and the pupil size can fluctuate from 10diameter. The visual surface of the iris is shaped amid fetal growth and balances out amid the initial two years of life. Nonetheless, the pigmentation, keeps evolving. The mind boggling iris surface contains many interweaving minute qualities, for example, coronas, spots, crypts, and so forth which are all different for every individual.

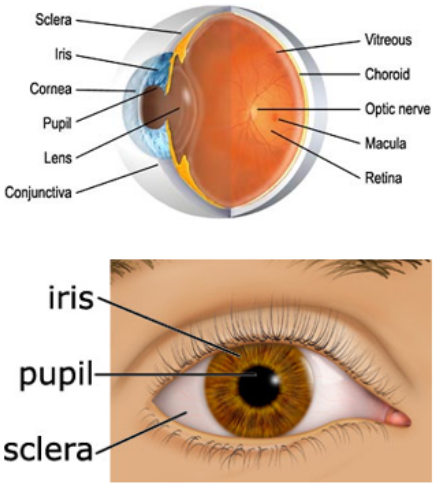

Figure 1.1: Anatomy of human eye

1.2 Operations Performed on Acquired Iris Image

The exactness and speed of presently used iris-based acknowledgment frameworks is promising and bolster the plausibility of extensive scale recognizable proof frameworks in view of iris data. Each iris is particular and even the irises of indistinguishable twins are distinctive.

The iris in the figure needs to be found out so that subsequent post-processing techniques can be carried out. In the event that iris and pupil limits are roundabout, subsequently the limit of circle can be depicted with the parameters:

1. radius r,
2. center of the circle (x_0, y_0),

Three principle ventures are to be performed for doing iris recognition, which include: Segmentation, Normalization, and Feature Encoding and Matching.

The project work is performed mostly on the segmentation of the eye image.

Figure 1.2: Acquired iris image sample from UBIRISv1 dataset

1.2.1 Iris Segmentation

The process of iris recognition starts with searching for an iris in the acquired image, outlining its interior boundary at pupil and what's more, external boundary at sclera. Then we distinguish the upper eyelid and lower eyelid limits in the event that they impede, and distinguishing and omit out any superimposed eyelashes, or reflections from the lens worn. These procedures may altogether be called segmentation of the eye image. Images may not be suitable for segmentation right away, and might need to be enhanced by image enhancement algorithms so that certain post-processing techniques can be carried out properly.

Figure 1.3: Iris Localization

1.3 Motivation

Iris recognition is currently a popular area of research. One of the most important stages of the iris recognition is the segmentation stage. If an image is not correctly segmented, it can't be properly processed later on to find the appropriate iris code. There are several challenges in iris segmentation which include specular reflections due to glasses, non-circular pupillary and iris boundaries, occlusion due to eyelids and eyelashes, defocusing, motion blur or poor contrast. For solving these challenges, heavy computational resources may be required. To find out a solution of these problems which is less computationally intensive, is what motivated this research work.

1.4 Objective

The objectives of this project include:

i) Understand Iris recognition process.

ii) Gather iris images from UBIRIS iris image database.

iii) Carry out segmentation process for the iris images.

iv) To define four points C1, C2, C3 and C4 where the iris intersects with the eyelids and define the curves joining these points.

1.5 Dataset Description

The experiment has been carried out on UBIRIS dataset [2, 3]. It consists images of 1877 in number from 241 persons. There are images of different degrees of noise. Images are in 24 bit color format. Segmentation process if successful on these images would be robust and can be easily extended to other datasets like Multimedia University (MMU) iris database or CASIA database.

Dataset Name	No. of images	No. of classes	Images per class	Pixel Dimensions
MMU Version 1.0	450	90	5	320 X 240
UBIRIS.v1	1877	241	1-9	200 X 150
CASIA-Iris-Interval	2639	395	1-26	320 X 280

Table 1.1: Collected Dataset attributes

1.6 Related Work

Segmentation of the iris alludes to the procedure of naturally identifying the inner and outer limits of an iris in a given eye image. This procedure helps in feature extraction from the

distinctive surface of the iris. Iris segmentation assumes a key part in the execution of an iris detection and recognition framework. Hough Transform is utilized to find the points of interest. Here the feature extraction is performed with the help of Laplacian of Gaussian filters at various resolutions. Then, the Hough transform strategy is associated to confine the boundaries of iris.

Daugman used his integro-differential operator [4] with a specific end goal to confine eyelid boundaries as a parabola; the circular shape used in Hough transform was changed to a parabolic path. Wildes [5] also used the parabolic curves to confine the upper eyelid and lower eyelid limits. The parabolic Hough change has been utilized to discover eyelid limits on the edge map. Masek [6] utilized the linear Hough transform as a method for restricting the upper and lower eyelids. Horizontal lines are used in this technique to separate eyelid regions. These intersect with the nearest points with regards to the pupil on the outer iris limit.

Some famous iris segmentation methods:

- **Daugman's integro-differential operator:**

  Here a smoothing function $G(r)$ is used over the image of the eye I(x, y). This method searches all around the image area (x, y) for the most extreme value in the blurred partial derivative with respect to gradually incrementing radius r over the normalized contour integral of I(x, y). 'ds' is circular arc on this integral, 'r' denotes the radius and (x_0, y_0) are the center coordinates.

$$\max_{r,x_0,y_0} \left| G_\sigma(r) \frac{\partial}{\partial r} \oint_{r,x_0,y_0} \frac{I(x,y)}{2\pi r} ds \right| \tag{1.1}$$

- **Wildes method:**

  To start with, a binary edge map format(bmp) of the image source is found out. Certain contour arguments are selected by the vote of edge points. It uses a gradient based edge identification technique for the outer iris/sclera boundary and inner iris and pupil boundary. A histogram based way is used to deal with local minima issues that may get involved with the gradient based technique. For the support of different ranges of the radius, slopes of image intensities are weighted. The next stage uses the notable circular Hough transform. It relies on threshold amounts of edge maps for the given input iris image.

- **Libor Masek's method:**

  Here Masek[6] proposes a strategy that starts with the binary edge map construction which utilizes the Kovesi edge indicator, a variety of the already known Canny edge detection[7] technique for finding the iris and sclera boundary. It uses different

weight for vertical gradient and horizontal gradient. It uses circular Hough transform technique[8] to detect the inner pupil and outer iris boundaries. This procedure can be used for various image intensites.

- **Active Contour method:**

  Dynamic contour models were made use of by Ritter et al. [10] for restricting the pupil in acquired eye images. These contours react to inward forces and outside forces which are previously set upon. They change shapes by twisting inside or moving over a figure until balance is retained. Number of vertices are present in the contour , whose positions are changed by two forces which are of opposite in nature. Internal force is subject to the certain attributes which are desired, and the outer force is subject to the acquired image. The vertex keeps on changing with respect to time. If one wants to localise the pupil sectors, the interior powers are tuned as per convenience so that the an all inclusive extending discrete circle is formed. The edge points information provide us with exterior forces. Variance image is used in this technique. This discrete contour is regulated due to the external and internal forces for localising the pupil boundary.

- **Other methods:**

  The circular Gabor channel (CGF) [11, 12] has been used with a specific end goal to restrict the underlying pupil focus. The principle preferred standpoint of this approach is that the segmentation process for both the pupil and in addition the iris limits is successfully carried out. In this approach, a various high order nearby pixel dependencies is used which utilizes Zernike moments (ZM), so as to perfectly group the eye area pixels into iris. The non iris areas utilize the trained neural system/support vector machine (NN/SVM) classifiers. Image improvement technique which uses single scale retinex (SSR) calculation has been utilized for internsity variation issue.

Some eyelid detection methods:

The detection of upper and lower eyelids includes the scan for two curves, which fulfill the polynomial equation :

$$y(x) = ax^2 + bx + c,\ x \in [0, 1] \tag{1.2}$$

By checking the change for each square, we are able to recognize the eyelashes. Some others have likewise utilized minimum threshold basis ways to deal with locating the coarse boundaries of pupil. Thresholding over the intensity values in the pupil area separates its boundary.

- **Eyelash detection by Kong and Zhang:**

  A technique for the location of eyelashes was proposed by Kong and Zhang[13]. He classified the eyelashes into separable eyelashes, which can be effectively isolated

from the figure and multiple eyelashes, which can be clustered together and coincide in the eye image. To identify detachable eyelashes, 1-D Gabor filters are used. These give a low yield value for the separable eyelashes. Accordingly, data points less than a threshold determine the eyelash points. Variation of intensity technique is utilized for identifying multiple eyelashes.

- **Isolation of eyelids by Libor Masek:**

  In [6], Masek used Linear Hough transform[9] in confining the occlusion by eyelids and are isolated. It uses a different horizonal line that intersects with the previous line, allowing for maximum isolation of the eyelids. On the off chance that the in Hough space is lower than a set limit, at that point no line is fitted, since this compares to non-blocking eyelids.

- **Radman's live-wire method**

  A. Radman et al.[14] proposed a technique for eyelid detection. It uses a live-wire technique in which edge detector is utilized to filter the external iris boundary and calculate the average estimation of the contiguous pixels for every pixel on the external iris boundary; As soon as the average estimate surpasses the threshold value at a specific pixel, this pixel is considered as a intersection point between the eyelid and the external iris boundary.

1.7 Experimental Setup

All the procedures applicable to the thesis are run on 2.4GHz Intel(R) Core(TM) i5-6200U CPU quad core processor with 8GB RAM. The process is simulated using MATLAB® Version 8.0.0.783(R2012b).

1.8 Thesis Layout

The thesis consists of 3 chapters. The remaining part of the thesis include

- In chapter 2, segmentation of iris images are carried out using circular Hough transform, upper and lower eyelid detection is done and a method is proposed for finding out the intersection points of the iris outer boundary with the eyelids. Sample implementation results are shown.

- In chapter 3, implementation results of the operations performed are shown for a sample of 25 images of different persons. All the attributes required to characterize the eye shape are defined here.

- In chapter 4, conclusion of the research project work is done along with future prospective research options are provided.

Chapter 2

Proposed Scheme

2.1 Proposed Methodology

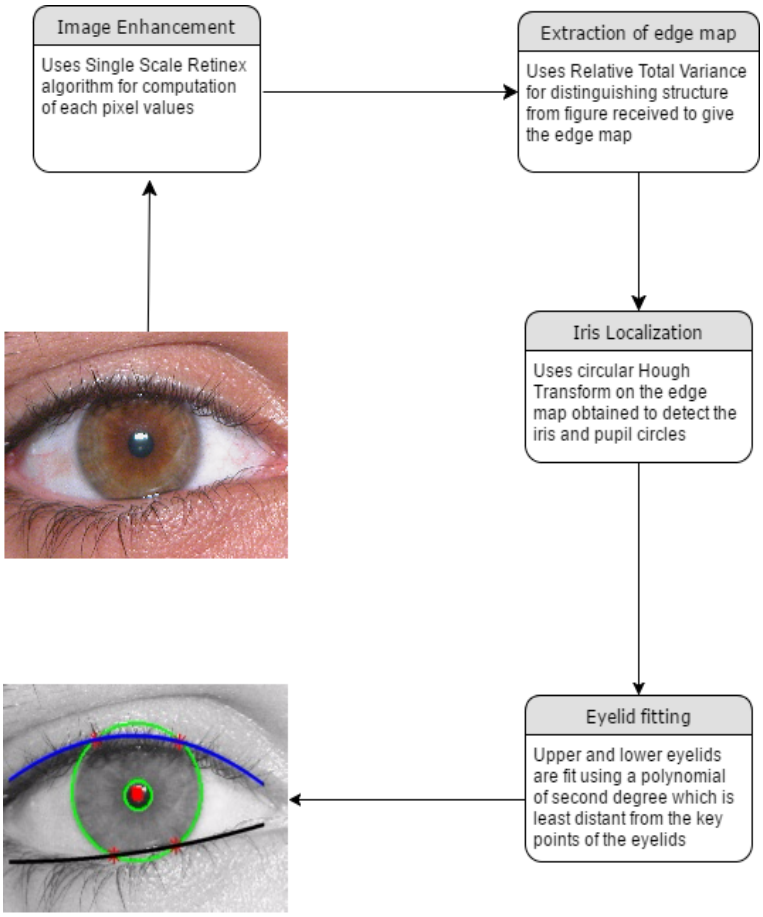

Figure 2.1: Methodology Flow Chart

Iris segmentation alludes to the procedure of consequently finding the annular locale included between the pupillary and limbic limits of the iris in a given figure. The segmentation process is thought to be of vital significance in iris recognition. This is on account of mistakes in segmentation can essentially bring down the performance of iris recognition. The operations performed in the proposed methodology overview are carried out on the acquired iris images.

2.2 Image Enhancement

Specular reflection evacuation: Specular reflections are little areas in an iris image described by pixels of high intensity rates. Such reflections are commonly created by unconventional centering of the light source. Iris segmentation is considered challenging if specular reflections are available near the iris boundary limits. These areas are referred to as noise, along these lines bringing down the operation performance. Hence, we first concentrate on dealing with specular reflections. To solve these issues of illumination intensity and varying angles of the light source, we use the Single Scale Retinex(SSR) algorithm [15]. This algorithm re-computes each pixel's intensity value for each of the RGB channel using the formula:

$$S_{i\in\{R,G,B\}}(x,y) = \log \frac{I_i(x,y)}{G_\sigma * I_i(x,y)} \tag{2.1}$$

where I_i is the given input eye image on the respective channel i, G_σ corresponds to the Gaussian kernel which has a standard deviation σ, and the symbol $*$ denotes convolution. A median filter is applied on this enhanced image so as to smooth some of the noise areas in the image, thereby influencing consequent processing. We set the size of the Gaussian kernel as 300 and set median filter size to 7.

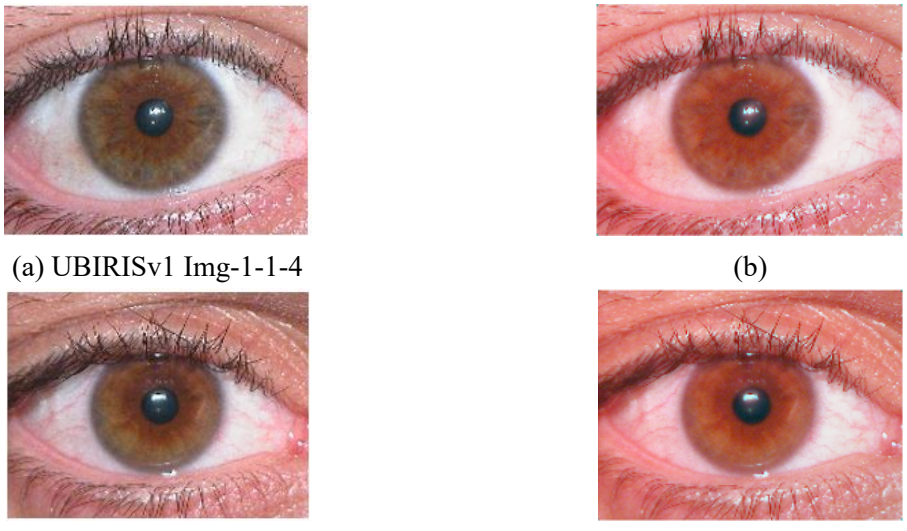

(a) UBIRISv1 Img-1-1-4 (b)

(c) UBIRISv1 Img-2-1-1 (d)

Figure 2.2: SSR enhanced images for UBIRISv1 images

2.3 Extraction of edge map

One normal trademark for iris images of visible wavelength is they are susceptible to noise, reflection and eyelashes, which are not required in the underlying structure examination. Thus generally used integro - differential operator and Circular Hough Transform (CHT) can't be utilized straightforwardly these images, in light of the fact that both techniques require clear contrast at these structure segments and slightest impedance from noise. Relative Total Variance (RTV) depicted in [16] has indicated great capacity to recognize structure from surface in a figure. This technique may help in drawing out the fundamental structure of iris to get an effective outcome.

The edge outline of the iris figure is drawn out utilizing Relative Total Variance map. RTV can recognize structure from figure appropriately. This system utilizes a blend of windowed total variation D and windowed inherent variation L. At long last, weights are added to two steerings of the inherent variation term L, so this weighted local total variation term can help in distinguishing upper and lower bends of the eye which might be covered. It helps in extracting the eye structure which can be utilized as a part of finding out the exact boundaries of iris in next stage. The nature of such structure map is extraordinary on the grounds that the curve of the circle is plainly obvious, and conceivable impedance from various portions, for example, surface edges and eyelid is minor. This impact can't be attained by tuning threshold values of essential edge locators.

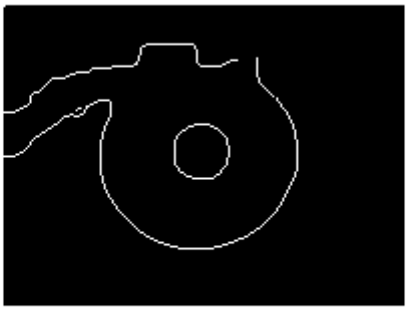

Figure 2.3: Sample extracted edge map

2.4 Iris Localization

Pupillary and limbus limit identification: The core of an iris segmentation technique is to distinguish the pupillary and pupil limits of the iris. Most segmentation techniques are demonstrated by accepting these limits to be round. Such supposition remains constant in

this experiment as well. This district can then be utilized as a beginning stage for the outward spread pursuit of the limbus limit. Then again, most visible wavelength iris segmentation approaches intend to estimate the pupillary limit first because of the significant edge response between the iris and sclera, and less significant edge response between the iris and pupil in lightly shaded iris images. The area inside the limbic boundary is then utilized for a scan of the pupillary boundary.

Circle detection

The CHT based approach is altered to identify iris circle on the extracted edge outline. But image occlusion may happen because of upper-half circle of iris being covered by eyelid. We fix the scope of probable radius $[r_s, r_l]$, and set it to [35, 120]. r ranges within these values. Let (x_c, y_c) is approximately the center of a circle and (x_p, y_p) is roughly the center of pupil circle. p is the pupil region. S is the drawn out image region.

Normal Circular Hough Transform technique particularly utilizes the focal center recognized before to find the radius. So as to enhance the segmentation procedure, the center point is re-looked inside little area around the given focal center. The detection of iris and pupil circle is accomplished via looking for a circle with most extreme response, which utilizes the equation:

$$M = \arg\max_{x_i, y_i, r} \sum_{p \in S} H(x_i, y_i, r, p)$$

where

$$H(x_i, yi, r, p) = \begin{cases} 1, & \text{if } (x_i - x_p)^2 + (y_i - y_p^2) = r^2 \\ 0, & \text{otherwise} \end{cases} \tag{2.2}$$

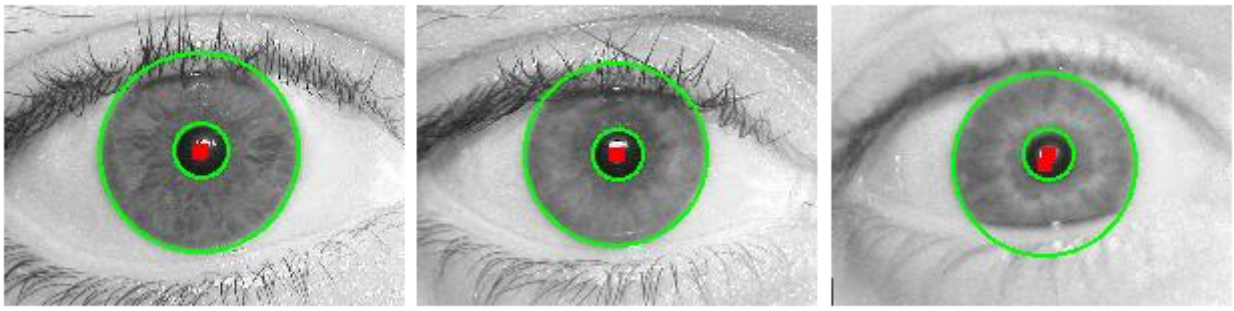

Figure 2.4: Sample localized eye images

2.5 Eyelid Fitting

We use the weighted local total variation model used in circle detection to detect and fit the upper and lower eyelids. We add a small weight λ in the weighted total variation map W_λ,

which would give us the vertical slope inclination data and smother the level slope. We set λ to 0.25 and experiment with the fitting. The approach used in [17] is utilized for the fitting procedure. It utilizes a polynomial of second degree to fit the eyelid. One can expect good functioning from this technique. Our main objective is to, as far as possible detect and limit the key points from the edge map outline, which was obtained in circle detection stage, to a rectangle area B, which is characterized as:

$$B = (x_i, y_i) \Big| x_o - r_{ic} \leq x_i \leq x_i + r_{ic}, y_o - r_{ic} \leq y_i \leq y_i + 0.3 * r_{ic} \tag{2.3}$$

where (x_o, y_o) is the center point of iris circle and r_{ic} is the radius of it. The key points are found from the edge map that are inside B region but outside pupil region. These points are right off the bat regarded as a decent representation of the eyelid. At that point a two-stage method is done to fit the eyelid outline to a polynomial of second degree using the formula: the polynomial equation :

$$y(x) = ax^2 + bx + c, \; x \in [0, 1] \tag{2.4}$$

As we would be defining three points within the region B, and trying different combinations of these points for trying to find the best polynomial that would fit these key points, we can take a polynomial of second degree as above and try to fit them. No prior training is needed for this type of model in trying to detect the eyelid points. These models are adaptively built by using the data we get from localizing iris boundary.

- A rectangular box of all the key points within B region is obtained using above equation. The following points are calculated where:

  (x_{mid}, y_{mid}): center of B ; (x_s, x_l): furthest left x-coordinate and furthest right x-coordinate of B; y_{min} : least y-coordinate of B . At this point, three polynomials having order of second degree are fixed and created which cross following arrangement of points individually:

  1. $\{ (x_s, y_{min}), (x_{mid}, y_{mid}), (x_l, y_{min}) \}$,
  2. $\{ (x_s, y_{min}), (x_{mid}, y_{mid}), (x_l, y_{mid}) \}$, and
  3. $\{ (x_s, y_{mid}), (x_{mid}, y_{mid}), (x_l, y_{min}) \}$.

  From the given three polynomials constructed using the 'polyfit' method in MATLAB®, we use the one that gives the least d_i distance to the key points that are maintained. The other two polynomials won't be used any further and are disposed.

- This single polynomial obtained works as a threshold. It keeps those key points which follow the conditions:

$$\frac{(d_{ij} - \mu_d)^2}{\sigma_d^2} > 3 \tag{2.5}$$

where μ_d is the mean of all the d_i distances from key edge points to the final polynomial and σ_d standard deviation of it. d_{ij} represents the d_i distance of any point j. Here the value '3' serves as the max threshold for qualified key edge points.

As per this formula, it is guaranteed that the edge points are not very far from the obtained second degree polynomial. The developed algorithm is robust and found to be highly effective for images acquired under less-constrained imaging. Similarly, for lower eyelid ranges are changed to $[0.8, 1]$ and lower eyelid curve is found out.

2.6 Intersection of curves

After the curves of lower eyelid, upper eyelid and the circle boundaries are obtained, we plot these and try to find the intersections of the points using curve intersection technique [18] or plot the curves and the circle and check if there are points where the difference between the curve points are less than a relatively very small value. Coordinates obtained are stored in '.mat' format along with radius of iris circle, radius of pupil circle, center of circle and coefficients of the polynomials obtained.

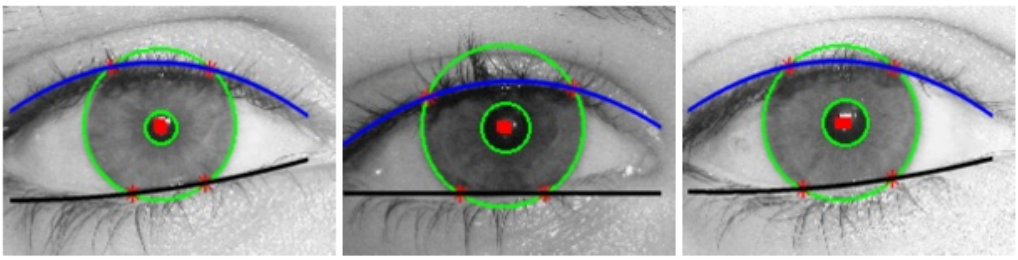

Figure 2.5: Final image after eyelid fitting operations

Chapter 3

Implementation Results

If there are no intersection point at upper eyelid, then we set the points C1 and C2 to $(0, 0)$. Similarly, C3 and C4 are set to $(0, 0)$, if no intersection point obtained at lower eyelid. We set all the points, i.e. , C1, C2, C3 and C4 to $(0, 0)$, if no intersection points obtained.

The experiment was carried out on 1876 images. As it won't be feasible to write all the attributes of each image, the attributes obtained from segmenting 25 sample images are stated below.

UBIRIS Image Name	Iris center	Iris radius	Pupil center	Pupil radius
Img-1-1-1	(102, 76)	49	(104, 75)	12
Img-2-1-1	(100, 75)	45	(101, 75)	12
Img-3-1-5	(107, 80)	45	(109, 75)	12
Img-4-1-2	(104, 69)	48	(106, 72)	13
Img-5-1-3	(98, 73)	43	(101, 71)	14
Img-6-1-1	(97, 72)	49	(88, 80)	17
Img-7-1-2	(107, 72)	46	(108, 70)	11
Img-8-1-3	(101, 78)	47	(102, 78)	14
Img-9-1-2	(106, 75)	45	(108, 75)	13
Img-10-1-2	(100, 78)	47	(101, 77)	11
Img-11-1-5	(98, 80)	47	(99, 77)	14
Img-12-1-1	(95, 78)	48	(97, 79)	11
Img-13-1-2	(101, 73)	43	(102, 71)	14
Img-14-1-3	(97, 75)	45	(99, 73)	11
Img-15-1-4	(91, 81)	47	(93, 79)	12
Img-16-1-3	(102, 78)	45	(105, 77)	12
Img-17-1-2	(103, 70)	46	(106, 69)	13
Img-18-1-5	(90, 69)	49	(92, 71)	13
Img-19-1-3	(104, 79)	45	(105, 81)	13
Img-20-1-1	(104, 79)	43	(108, 78)	10
Img-21-1-5	(95, 76)	47	(97, 75)	13
Img-22-1-2	(100, 74)	46	(101, 74)	12
Img-23-1-3	(105, 76)	43	(107, 74)	10
Img-24-1-3	(104, 70)	44	(105, 67)	13
Img-25-1-4	(87, 67)	46	(88, 67)	12

Table 3.1: Iris circle and pupil circle properties for sample eye images from UBIRISv1 dataset

Equation $y(x) = ax^2 + bx + c$			
UBIRIS Image Name	a	b	c
Img-1-1-1	0.0035	-0.8062	73.0241
Img-2-1-1	0.0015	-0.3136	59.9885
Img-3-1-5	0.0008	-0.3019	55.9492
Img-4-1-2	0.0007	-0.1247	56.4087
Img-5-1-3	0.0008	-0.2810	61.3462
Img-6-1-1	0.0021	-0.3990	66.5325
Img-7-1-2	0.0007	-0.2984	64.5280
Img-8-1-3	0.0053	-1.0745	85.2606
Img-9-1-2	0.0008	-0.2509	58.7959
Img-10-1-2	0.0015	-0.5269	74.1934
Img-11-1-5	0.0059	-1.0655	88.6215
Img-12-1-1	0.0036	-0.6648	60.7066
Img-13-1-2	0.0048	-1.0356	103.3018
Img-14-1-3	0.0008	-0.1168	46.3477
Img-15-1-4	0.0007	-0.1158	49.9413
Img-16-1-3	0.0046	-1.0016	87.2851
Img-17-1-2	0.0015	-0.5140	71.1028
Img-18-1-5	0.0007	-0.1231	34.5442
Img-19-1-3	0.0138	-2.9326	192.4593
Img-20-1-1	0.0032	-0.7662	89.8629
Img-21-1-5	0.0015	-0.1868	46.3162
Img-22-1-2	0.0030	-0.5290	51.4867
Img-23-1-3	0.0008	-0.2780	66.0479
Img-24-1-3	0.0039	-0.7620	84.8342
Img-25-1-4	0.0007	-0.0703	34.3855

Table 3.2: Iris upper eyelid curve coeffs. for sample eye images from UBIRISv1 dataset

Equation $y(x) = ax^2 + bx + c$			
UBIRIS Image Name	a	b	c
Img-1-1-1	-0.0021	0.4625	96.0369
Img-2-1-1	-0.0008	0.2912	96.8108
Img-3-1-5	-0.0056	1.1889	61.3944
Img-4-1-2	0	0	109.7368
Img-5-1-3	-0.0058	1.1395	60.1628
Img-6-1-1	-0.0035	0.6649	85.9545
Img-7-1-2	-0.0060	1.3117	44.0164
Img-8-1-3	0	0	121.5263
Img-9-1-2	-0.0054	1.1619	54.8143
Img-10-1-2	0	0	118.6842
Img-11-1-5	-0.0007	0.2322	106.5724
Img-12-1-1	0	0	124.9474
Img-13-1-2	0	0	116.5263
Img-14-1-3	-0.0056	1.0778	67.7278
Img-15-1-4	-0.0007	0.2715	107.7847
Img-16-1-3	0	0	122.7368
Img-17-1-2	-0.0007	0.0165	119.3303
Img-18-1-5	0	0	110.7895
Img-19-1-3	0	0	118.5789
Img-20-1-1	-0.0024	0.5535	88.4852
Img-21-1-5	-0.0029	0.5717	91.3638
Img-22-1-2	-0.0007	0.1464	107.2217
Img-23-1-3	-0.0058	1.2209	54.9012
Img-24-1-3	-0.0071	1.4353	39.3018
Img-25-1-4	-0.0054	0.9457	71.8641

Table 3.3: Iris lower eyelid curve coeffs. for sample eye images from UBIRISv1 dataset

UBIRIS Image Name	C1(x,y)	C2(x,y)	C3(x,y)	C4(x,y)
Img-1-1-1	(85.82, 29.75)	(105.39, 27.14)	(79.39, 119.44)	(121.13, 121.08)
Img-2-1-1	(65.60, 46.01)	(133.94, 45.48)	(79.70, 115.15)	(107.87, 119.30)
Img-3-1-5	(0, 0)	(0, 0)	(0, 0)	(0, 0)
Img-4-1-2	(59.31, 51.54)	(149.53, 53.83)	(78.65, 109.73)	(129.38, 109.73)
Img-5-1-3	(64.03, 46.64)	(124.07, 38.83)	(0, 0)	(0,0)
Img-6-1-1	(52.56, 51.39)	(141.89, 52.43)	(75.73, 116.1)	(120.49, 114.98)
Img-7-1-2	(67.95, 47.71)	(137.58, 37.66)	(84.17, 111.92)	(125.18, 114.23)
Img-8-1-3	(0, 0)	(0, 0)	(83.30, 121.52)	(118.67, 121.52)
Img-9-1-2	(72.85, 44.58)	(132.94, 38.98)	(85.16, 114.86)	(123.24, 116.53)
Img-10-1-2	(65.68, 45.91)	(114.11, 33.17)	(76.46, 118.68)	(123.48, 118.68)
Img-11-1-5	(68.97, 43.05)	(135.91, 52.23)	(72.68, 119.57)	(115.48, 123.60)
Img-12-1-1	(0, 0)	(0, 0)	(85.02, 124.94)	(104.88, 124.94)
Img-13-1-2	(60.62, 58.20)	(138.63, 52.21)	(0, 0)	(0, 0)
Img-14-1-3	(66.47, 41.96)	(129.69, 44.08)	(0, 0)	(0, 0)
Img-15-1-4	(60.05, 45.63)	(123.22, 46.80)	(70.48, 123.27)	(98.41, 127.39)
Img-16-1-3	(93.32, 33.85)	(101.29, 33.00)	(97.34, 122.73)	(106.81, 122.73)
Img-17-1-2	(65.04, 44.01)	(125.93, 30.15)	(91.61, 114.54)	(126.75, 109.37)
Img-18-1-5	(60.81, 29.65)	(119.46, 29.87)	(64.45, 110.78)	(115.56, 110.78)
Img-19-1-3	(61.49, 64.28)	(140.52, 52.74)	(82.63, 118.57)	(125.40, 118.57)
Img-20-1-1	(70.80, 51.69)	(129.54, 44.43)	(86.81, 118.39)	(115.85, 120.31)
Img-21-1-5	(64.35, 40.37)	(132.15, 47.25)	(72.88, 117.44)	(115.55, 118.24)
Img-22-1-2	(94.98, 28.29)	(113.79, 30.12)	(77.41, 114.06)	(122.86, 113.89)
Img-23-1-3	(70.44, 50.44)	(132.85, 43.26)	(0, 0)	(0, 0)
Img-24-1-3	(63.77, 52.17)	(146.05, 57.13)	(88.06, 110.99)	(125.65, 108.27)
Img-25-1-4	(56.26, 32.80)	(121.80, 36.94)	(0, 0)	(0, 0)

Table 3.4: Iris image curve intersection points for sample eye images from UBIRISv1 dataset

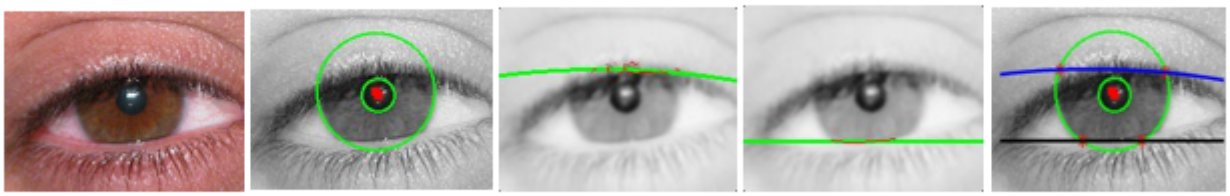

Figure 3.1: Characterizing eye image Img-4-1-2.jpg: 4 intersection points.

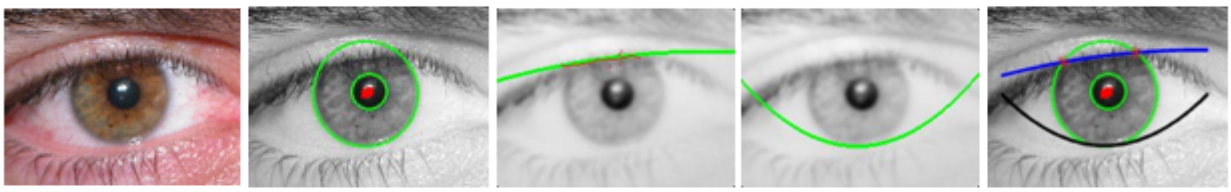

Figure 3.2: Characterizing eye image Img-5-1-3.jpg: 2 intersection points on upper eyelid.

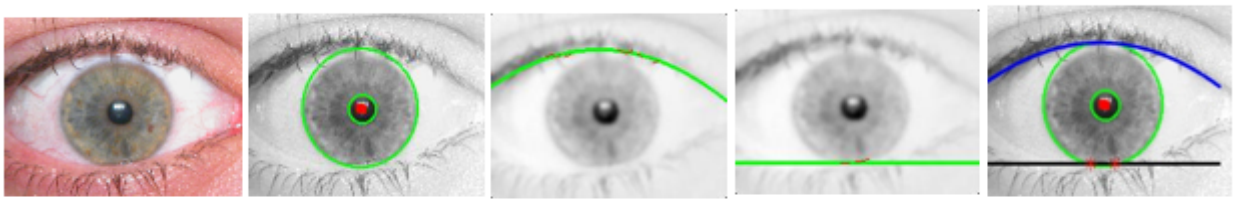

Figure 3.3: Characterizing eye image Img-12-1-1.jpg: 2 intersection points on lower eyelid.

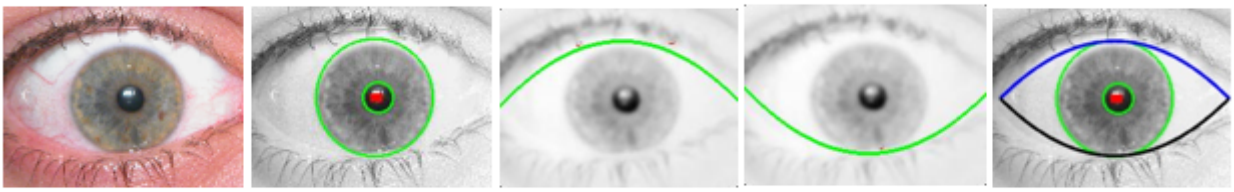

Figure 3.4: Characterizing eye image Img-12-1-3.jpg: 0 intersection point.

Chapter 4

Conclusion

We are able to successfully segment noisy visible wavelength iris images efficiently. We are able to use the total variation model to approximately extract the primary structure around the iris boundary area. We are able to define the iris region using the equation from the upper eyelid and lower eyelids. C1 and C2 intersection points are obtained from the intersection of curves - localized iris boundary and upper eyelid. Similarly, C3 and C4 intersection points are obtained from the intersection of curves - localized iris boundary and lower eyelid.

The total variation model used in extracting the primary structure is also used in eyelid fitting. The grayscale attributes of the eyelid edge are utilized to restrict the edge points. The edge of the eyelid is found approximately. The eyelid location calculation lessens the 3-D search space to 1-D to clearly enhance the search speed.

Scope for Further Research

The proposed technique uses circles for trying to localize the iris and pupil boundaries. It can further be extended to use active contour techniques to compare them with the respective points obtained after intersection with the eyelid curves obtained.

References

[1] Jain, A. K., Flynn, P., and Ross, A. A., 2007. *Handbook of Biometrics*. Springer-Verlag New York, Inc., Secaucus, NJ, USA.

[2] Ubiris.v1 database, `http://iris.di.ubi.pt/ubiris1.html`.

[3] Proença, H., and Alexandre, L., 2005. "Ubiris: A noisy iris image database". *Image Analysis and Processing–ICIAP 2005*, pp. 970–977.

[4] Daugman, J. G., 1993. "High confidence visual recognition of persons by a test of statistical independence". *IEEE Trans. Pattern Anal. Mach. Intell.,* **15**(11), Nov., pp. 1148–1161.

[5] Wildes, R. P., 1997. "Iris recognition: an emerging biometric technology". *Proceedings of the IEEE,* **85**(9), Sep, pp. 1348–1363.

[6] Masek, L., 2003. Recognition of human iris patterns for biometric identification. Tech. rep., University of Western Australia.

[7] Canny, J., 1986. "A computational approach to edge detection". *IEEE Transactions on Pattern Analysis and Machine Intelligence,* **PAMI-8**(6), Nov, pp. 679–698.

[8] VC, H. P., 1962. Method and means for recognizing complex patterns, Dec. 18. US Patent 3,069,654.

[9] Duda, R. O., and Hart, P. E., 1972. "Use of the hough transformation to detect lines and curves in pictures". *Communications of the ACM,* **15**(1), pp. 11–15.

[10] Ritter, N., Owens, R., Cooper, J., and Van Saarloos, P. P., 1999. "Location of the pupil-iris border in slit-lamp images of the cornea". In Image Analysis and Processing, 1999. Proceedings. International Conference on, IEEE, pp. 740–745.

[11] Radman, A., Jumari, K., and Zainal, N., 2012. "Iris segmentation in visible wavelength environment". *Procedia Engineering,* **41**, pp. 743–748.

[12] Ma, L., Wang, Y., and Tan, T., 2002. "Iris recognition using circular symmetric filters". In Object recognition supported by user interaction for service robots, Vol. 2, pp. 414–417 vol.2.

[13] Kong, W. K., and Zhang, D., 2001. "Accurate iris segmentation based on novel reflection and eyelash detection model". In Proceedings of 2001 International Symposium on Intelligent Multimedia, Video and Speech Processing. ISIMP 2001 (IEEE Cat. No.01EX489), pp. 263–266.

[14] Radman, A., Zainal, N., and Ismail, M., 2013. "Efficient iris segmentation based on eyelid detection". *Journal of Engineering Science and Technology,* **8**(4), pp. 399–405.

[15] Brainard, D. H., and Wandell, B. A., 1986. "Analysis of the retinex theory of color vision". *JOSA A,* **3**(10), pp. 1651–1661.

[16] Xu, L., Yan, Q., Xia, Y., and Jia, J., 2012. "Structure extraction from texture via relative total variation". *ACM Trans. Graph.,* **31**(6), Nov., pp. 139:1–139:10.

[17] Tan, C.-W., and Kumar, A., 2013. "Towards online iris and periocular recognition under relaxed imaging constraints". *IEEE Transactions on Image Processing,* **22**(10), pp. 3751–3765.

[18] Schwarz, D., 2017. Fast and robust curve intersections. University of Rochester, `http://in.mathworks.com/matlabcentral/fileexchange/11837-fast-and-robust-curve-intersections`.